Journal of Biomedical Optics

SPIEDigitalLibrary.org/jbo

In vivo observation of age-related structural changes of dermal collagen in human facial skin using collagen-sensitive second harmonic generation microscope equipped with 1250-nm mode-locked Cr:Forsterite laser

Takeshi Yasui
Makoto Yonetsu
Ryosuke Tanaka
Yuji Tanaka
Shu-ichiro Fukushima
Toyonobu Yamashita
Yuki Ogura
Tetsuji Hirao
Hiroyuki Murota
Tsutomu Araki

SPIE

In vivo observation of age-related structural changes of dermal collagen in human facial skin using collagen-sensitive second harmonic generation microscope equipped with 1250-nm mode-locked Cr:Forsterite laser

Takeshi Yasui,[a,b,c] Makoto Yonetsu,[a] Ryosuke Tanaka,[a] Yuji Tanaka,[a] Shu-ichiro Fukushima,[a,c] Toyonobu Yamashita,[d] Yuki Ogura,[d] Tetsuji Hirao,[d] Hiroyuki Murota,[e] and Tsutomu Araki[a]
[a]Osaka University, Graduate School of Engineering Science, 1-3 Machikaneyama, Toyonaka, Osaka 560-8531, Japan
[b]University of Tokushima, Institute of Technology and Science, 2-1 Minami-Josanjima, Tokushima 770-8506, Japan
[c]Nara Medical University, Graduate School of Medicine, 840 Shijo-cho, Kashihara, Nara 634-8521, Japan
[d]Shiseido Research Center, 2-2-1 Hayabuchi, Tsuzuki, Yokohama, Kanagawa 224-8558, Japan
[e]Osaka University, Graduate School of Medicine, 2-2 Yamadaoka, Suita, Osaka 565-0871, Japan

Abstract. *In vivo* visualization of human skin aging is demonstrated using a Cr:Forsterite (Cr:F) laser-based, collagen-sensitive second harmonic generation (SHG) microscope. The deep penetration into human skin, as well as the specific sensitivity to collagen molecules, achieved by this microscope enables us to clearly visualize age-related structural changes of collagen fiber in the reticular dermis. Here we investigated intrinsic aging and/or photoaging in the male facial skin. Young subjects show dense distributions of thin collagen fibers, whereas elderly subjects show coarse distributions of thick collagen fibers. Furthermore, a comparison of SHG images between young and elderly subjects with and without a recent life history of excessive sun exposure show that a combination of photoaging with intrinsic aging significantly accelerates skin aging. We also perform image analysis based on two-dimensional Fourier transformation of the SHG images and extracted an aging parameter for human skin. The *in vivo* collagen-sensitive SHG microscope will be a powerful tool in fields such as cosmeceutical sciences and anti-aging dermatology. [DOI: 10.1117/1.JBO.18.3.031108]

Keywords: nonlinear microscopy; second harmonic generation; collagen; dermatology; intrinsic aging; photoaging; tissue; dermis.

Paper 12412SSP received Jul. 1, 2012; revised manuscript received Nov. 6, 2012; accepted for publication Nov. 9, 2012; published online Dec. 5, 2012.

1 Introduction

Skin aging is one of the most interesting topics in the field such as cosmeceutical sciences and anti-aging dermatology, because skin is the superficial tissue of the human body and hence is always in public view. For middle-aged and elderly people, skin aging is definitely important matter as aesthetic facial concerns. Skin aging falls into the following two categories: intrinsic aging and photoaging.[1–3] The intrinsic aging as chronologic changes is caused by the declining fibroblast activity with aging as people get older and the subsequent decrease in dermal collagen fiber. The intrinsic aging is an irreversible, physiological phenomenon that cannot be avoided. For example, mechanical properties such as tension and elasticity decline gradually with age, resulting in the appearance of wrinkles and sagging. In a previous study, reduced synthesis of collagen fibers in chronologically aged skin was demonstrated, in which cellular fibroblast aging in the aged skin contributed to decreased type I and III collagen production.[4] In contrast, photoaging results from repeated exposure of the skin to ultraviolet (UV) rays in sunlight because UV irradiation causes dermal alterations, such as excessive secretion of matrix metalloproteinase (MMP) family, which degrades collagen and other extracellular matrix proteins,[5] and inhibition of procollagen biosynthesis resulting in a loss of collagen content.[6] These alterations lead to degenerately structural changes in the skin, such as leathery texture, laxity, and deep wrinkles.[7] Furthermore, repeated exposure to UV radiation even increases the risk of skin cancer.[8,9] As opposed to intrinsic aging, photoaging can be avoided by using sunshades and/or sunscreen creams.[10] Considering that skin aging appears as a result of both intrinsic aging and photoaging, the degree of skin aging is not always proportional to one's age but varies from individual to individual depending on the history of UV exposure as well as dietary intakes such as antioxidants.[11] Therefore, there is a need for an assessment technique for estimating the degree of skin aging.

The progress of skin aging is closely related to the dynamics of dermal collagen fibers because dermal collagen fibers contribute to the morphology and mechanical properties of the skin as a structural protein. The age-related structural change in dermal collagen has been extensively investigated based on histological methods of skin biopsy specimen. For example, morphometric examination of skin tissue section with optical microscope showed age-dependent change of quantity and diameter of

Address all correspondence to: Takeshi Yasui, University of Tokushima, Institute of Technology and Science, 2-1 Minami-Josanjima, Tokushima 770-8506, Japan. Tel: +81-886-656-7377; Fax: +81-886-656-7377; E-mail: yasui.takeshi@tokushima-u.ac.jp

collagen bundle in human skin.[12] However, such *ex vivo* assessment method of dermal collagen have often limited utility due to invasive skin biopsy. If *in vivo*, low-invasive assessment methods can be achieved, the application fields of the skin assessment method will be largely increased.

Among various inspection techniques for skin, optical probe methods are the most attractive for such *in vivo* assessments because they are simple, rapid, and low invasive. Furthermore, they can be applied directly because skin is a superficial tissue. Recent advances in ultrashort pulse lasers have opened the door to new optical probe methods based on optical nonlinear effects in biological tissue. When an ultrashort pulse of light is incident on a material with a noncentrosymmetric structure, light with half the wavelength of the incident light, known as second harmonic generation (SHG) light, is often produced via a nonlinear optical process.[13] Although the SHG process is widely used for wavelength conversion of laser light using a nonlinear optical crystal, it also enables unique collagen-sensitive microscope when applied to biological tissue.[14,15] This is because the SHG light is generated specifically by collagen molecules among various biological materials present due to the triple-helix structure of three polypeptide chains in this molecule. Collagen-sensitive SHG microscope provides unique imaging characteristics: high image contrast, high spatial resolution, optical three-dimensional (3-D) sectioning, low invasiveness, deep penetration, and no interference from background light. Most importantly, by using the naturally endogenous SHG process as a contrast mechanism, the structure of collagen fibers in tissue can be clearly visualized *in vivo* without additional staining.

Collagen-sensitive SHG microscope equipped with an 800-nm mode-locked Ti:Sapphire laser has been employed for *in vivo* visualizing of the dermal collagen fibers in mouse skin[16] and human skin.[17] Furthermore, European conformity-certified multiphoton microscope, giving two photon fluorescence (TPF) images of NAD(P)H, flavins, porphyrins, elastin, and melanin as well as SHG image of collagen, is commercially available for clinical instrument.[18] With respect to assessment of dermal photoaging, combined SHG and TPF microscope gives an indicator of changes in dermal collagen and elastin content *ex vivo*[19] and *in vivo*[20] because degradation of collagen and excessive deposition of abnormal elastin are observed in photoaged skin. Very recently, the elastin-to-collagen ratio has been introduced as a new indicator for human dermal skin aging.[21] On the other hand, a mode-locked Cr:F laser centered around 1250 nm has emerged as a new source for SHG microscope, showing decreased photodamage[22–24] and enhanced penetration depth.[25] The Cr:F laser-based SHG microscope has been successfully employed for imaging of dermal collagen fiber in excised mouse skin,[26] excised fixed human skin,[27] and *in vivo* human skin.[25,28] From the viewpoint of assessment of skin aging, since Cr:F laser-based SHG microscope enables us to probe down to deeper portions in the dermis-that is, the reticular dermis-it may contribute to a better understanding of age-related structural change in the dermal collagen fibers. For example, based on the fact that the efficiency of SHG light is sensitive to the collagen orientation when the incident light is linearly polarized, polarization-resolved, Cr:F laser-based SHG microscope has been applied to investigate the relation between wrinkle direction and collagen orientation in excised UV-exposed mouse skin.[29] However, few reports have revealed that aging-related structural changes in human dermal collagen fibers are clearly visualized *in vivo* in the form of high-contrast SHG images. In this article, Cr:F laser-based SHG microscope was used for *in vivo* visualization of aging-specific structural changes in human facial collagen. Furthermore, quantitative image analysis using Fourier transformation of SHG images was performed to identify characteristic structures in dermal collagen fibers with and without skin aging.

2 Materials and Methods

2.1 *Experimental Setup*

Figure 1(a) shows the experimental setup of our collagen-sensitive SHG microscope. Because the setup is described in detail elsewhere,[25,29] only a brief description of it is given here. A 1250-nm mode-locked Cr:Forsterite laser (Avesta Project Ltd., CrF-65P, pulse duration = 90 fs, mean power = 200 mW, repetition rate = 73 MHz) pumped by an Ytterbium fiber laser emitting at 1064 nm was used as a laser source. After converting the polarization of the laser light from linear to circular, the laser beam was scanned two-dimensionally by a pair of galvano mirrors (GM). After passing through relay lenses (RL1 and RL2), the laser beam was focused onto the sample with an objective lens (OL; Nikon Instruments Inc., CFI Plan $50 \times H$, magnification = 50, NA = 0.9, working distance = 350 μm, oil-immersion type). A customized attachment ring [see an inset of Fig. 1(a)] is attached to the subject's skin by a double-stick tape and used to suppress the motion of its measured position. By changing the position of the attachment ring with a stepping motor-driven translation stage, we can select the measured position inside the skin three-dimensionally. A portion of the generated SHG light was backscattered in the sample and then collected via the OL. The SHG light was descanned by GM and separated from the laser light by a harmonic separator (HS, reflected wavelength = 625 nm) and an infrared-cut filter (F, stop wavelength > 800 nm). The SHG light was detected by a photon-counting photomultiplier (PMT, Hamamatsu Photonics K. K., H8259-01) connected with a pulse counter.

Using the above GM optics, SHG images of a 600×600-μm region, composed of 256×256 pixels, were acquired at a rate of 2 s/image. However, this imaging region was not suitable for assessment of skin aging because the morphology and mechanical properties of the skin are influenced by the macroscopic properties of dermal collagen fiber rather than microscopic ones. To enlarge the imaging region, we scanned the sample position at intervals of 600 μm using a stepping motor-driven translation stage whenever acquiring SHG image of 600×600-μm regions using GM. Finally, we obtained a large SHG image with a size of 2.4×2.4 mm by arranging 16 SHG images in a matrix of four rows and four lines.

2.2 *Evaluation of Human Dermis*

Twelve Japanese male volunteers aged in their 20s to 60s with Fitzpatrick's skin phototype (SPT) III to IV were recruited as shown in Table 1. The cheek skin, serving as a sun-exposed site of healthy subjects, was assessed by using the SHG microscope as shown in Fig. 1(b) and 1(c). With respect to the question of risk of biological photodamage caused by the Cr:Forsterite laser, previous studies have reported that little damage was observed on zebrafish embryos[23] and hamster oral mucosa[24] after long-term irradiation with a tightly focused laser beam.

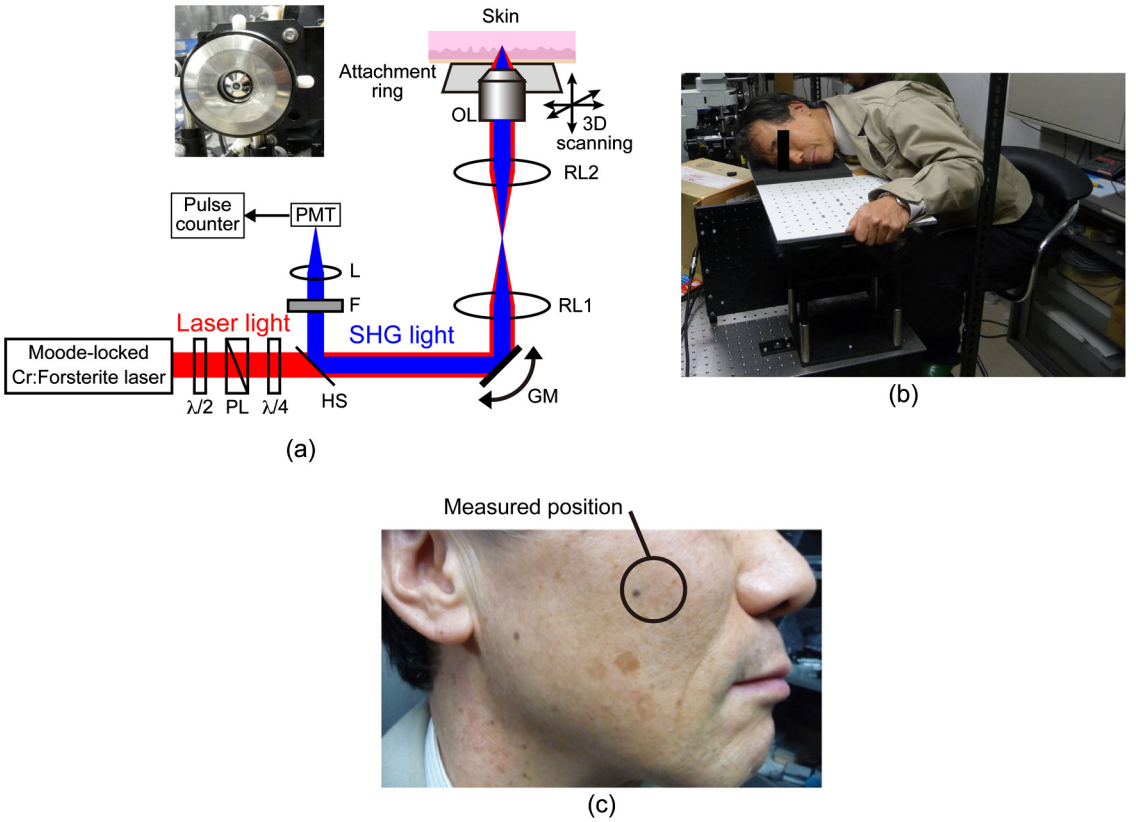

Fig. 1 (a) Experimental setup. $\lambda/2$: half waveplate; PL: polarizer; $\lambda/4$: quarter waveplate; HS: harmonic separator; F: infrared-cut filter; L: lens; PMT: photon counting-type photomultiplier tube; GM: galvano mirrors; RL1 and RL2: relay lenses; OL: oil-immersion objective lens. Photograph of (b) *in vivo* measurement and (c) measured position of human cheek skin.

Table 1 List of subjects.

Subject identifier	Sex	Age	History of sun exposure
A	Male	20s	Moderate
B	Male	20s	Moderate
C	Male	20s	Moderate
D	Male	20s	Excessive
E	Male	20s	Moderate
F	Male	30s	Moderate
G	Male	30s	Moderate
H	Male	40s	Moderate
I	Male	40s	Excessive
J	Male	50s	Excessive
K	Male	50s	Moderate
L	Male	60s	Moderate

Furthermore, to evaluate the risk of photodamage to human skin, we examined changes in the subjects' skin before, immediately after, and one month after irradiation with a laser light, based on color measurement with a spectrophotometer (Konica Minolta, CM-2600d) and clinical evaluation by a board-certified dermatologist. We concluded from these examinations that there was no laser-induced photodamage to the skin. Based on this evidence, we set the average power of the laser light radiated onto the skin to 35 mW with a combination of a half waveplate ($\lambda/2$) and a polarizer (PL). Written informed consent was obtained from all subjects before the measurement. The protocol conformed to the Helsinki Declaration and was approved by the ethics committees for human experiments in both Osaka University and Shiseido Co., Ltd.

3 Results and Discussions

3.1 *Structural Differences in Facial Collagen Fiber Among Subjects with Different Ages*

First we investigated differences in facial collagen fiber among male subjects with different ages. We set the probing depth to 200 μm from the skin surface to investigate the collagen fiber in the reticular dermis by performing depth-resolved SHG imaging before conducting the following experiments. Figure 2(a) to 2(e), respectively, show photographs of the cheek skin (image size $= 58 \times 43$ mm) and large-area SHG images (image size $= 2.4 \times 2.4$ mm) of a subject in his 20s (subject E), a subject in his 30s (subject G), a subject in his 40s (subject I), a subject in his 50s (subject K), and a subject

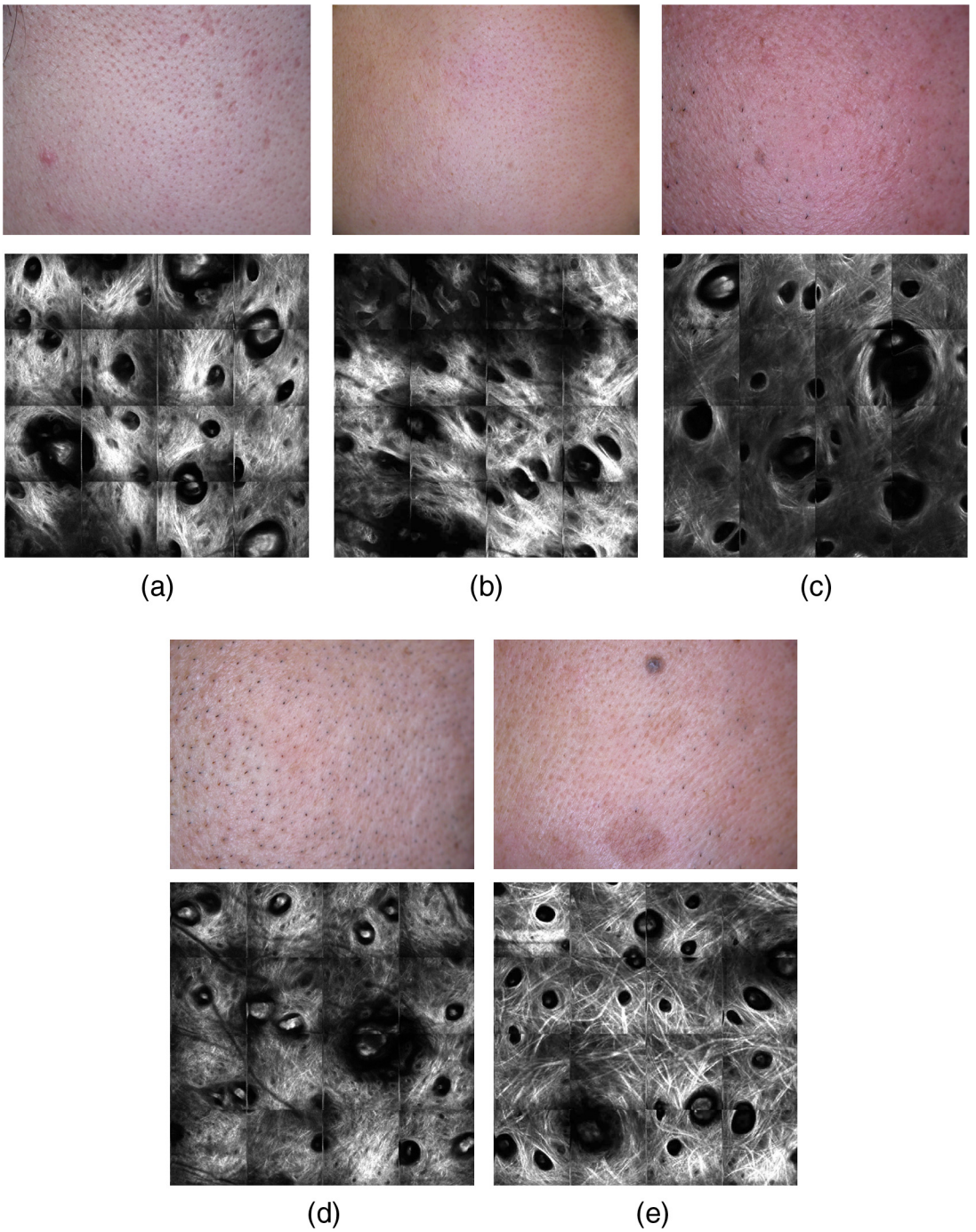

Fig. 2 Photographs of the cheek skin (image size = 58 × 43 mm) and large-area SHG images (image size = 2.4 × 2.4 mm) of (a) subject in his 20s (subject E), (b) subject in his 30s (subject G), (c) subject in his 40s (subject I), (d) subject in his 50s (subject K), and (e) subject in his 60s (subject L).

in his 60s (subject L). Imperfect matching of adjacent SHG images at the boundary is mainly due to a little discrepancy between the image region acquired by the galvano mirror and the movement of the stepping motor stage. In all SHG images, the detailed structure of dermal collagen fibers was clearly visualized. Although pores in the skin should appear as black circles due to the absence of collagen fiber, faint signals were observed in the centers of the pores, implying contamination of SHG image form other signals. We investigated the reason for this contamination by replacing the infrared-cut filter (pass wavelength <800 nm) with another optical filter with a sharp pass-band (pass wavelength = 590 to 630 nm) as shown in Fig. 3(a) and 3(b). The faint signals in the centers of the pores completely disappeared under insertion of the sharp pass-band filter. Although one possible reason for the false signals may be multiphoton autofluorescence from keratin[30] rich in the hair, it is difficult to specify the source of this faint signal at the present time.

Here we focus on structural differences in the dermal collagen fiber among subjects with different ages. For example, the skin of subject E indicated that thin collagen fibers were densely distributed [see Fig. 2(a)]. Conversely, in the case of subject L, thin collagen fibers were greatly reduced, and a coarse distribution of thickly grown collagen fibers was enhanced

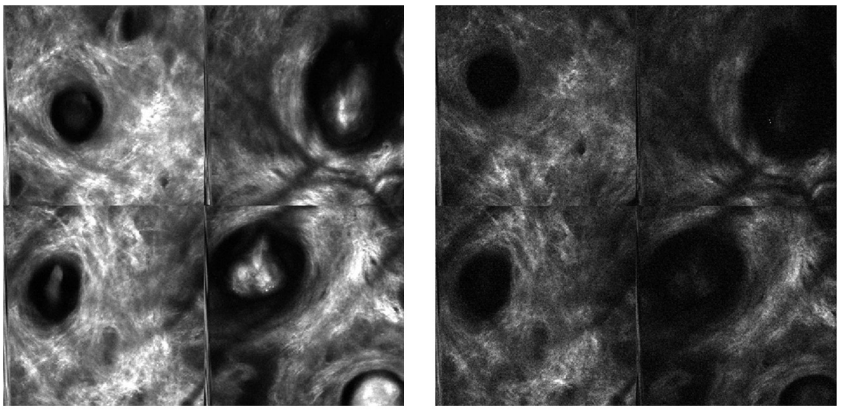

Fig. 3 Comparison of SHG image obtained with (a) the infrared-cut filter (pass wavelength <800 nm) and (b) sharp band-pass filter (pass wavelength = 590 to 630 nm).

[see Fig. 2(e)]. These age-related structural changes in dermal collagen fibers were confirmed in the previous studies. On one hand, *ex vivo* morphometric analysis of the reticular dermis indicated that fiber diameter in young subjects was thinner than that in elderly subjects.[12] On the other hand, confocal microscopy revealed *in vivo* that collagen bundles were abundant and composed of fine fiber in young subjects while the dermis showed coarse collagen and curled fibers in elderly subjects.[31] The thickness of a collagen fiber is closely related to the level of structural maturity in the fiber; immature fibers are thinner and mature fibers are thicker. Procollagen, which is collagen precursor molecule, is synthesized by dermal fibroblasts and secreted into extracellular spaces, where it is enzymatically processed to mature collagen. Mature collagen spontaneously forms fibrils, and then collagen fibrils build up their higher order structures, collagen fibers. Since collagen fibrils have an estimated half-life of 17 years, fragmented collagen fibrils accumulate with the passage of time.[5] This may lead to difference of SHG image between Fig. 2(a) and 2(e). Age-related decrease in collagen in the skin was also observed in the previous studies.[12,31] This good agreement with the previous studies indicates the high potential of SHG microscope for *in vivo* assessment of age-related change in dermal collagen fiber.

Regarding the skin of the subjects in their 30s, 40s, and 50s, we were expecting that the above structural changes in dermal collagen fiber would advance gradually in proportion to age. However, a series of SHG images in Fig. 2, from subjects in their 20s to 60s, did not always indicate such a gradual change. For example, the skin of the subject I in his 40s [see Fig. 2(c)] indicated a larger decrease of thin collagen fibers than in subject K in his 50s [see Fig. 2(d)]. We consider that photoaging influences these results because the effect of photoaging is not always in proportion to age, and individual subjects have different histories of UV exposure. Since males usually do not use sunshades or sunscreen creams carefully to avoid UV exposure, their skin will be susceptible to the effects of photoaging. Furthermore, subject I had a rich history of UV exposure by playing rugby football throughout the years, from elementary school to university. Although sun-protected part in the skin should be selected as a measurement position to investigate the intrinsic aging without the influence of photoaging, it is still interesting to visualize actual age-related structural change of facial collagen fiber *in vivo* from the viewpoint of aesthetic facial concerns and anti-aging dermatology. Work is in progress to conduct a similar experiment on female subjects. This is because females tend to use sunshades and/or sunscreen creams more carefully than males, and hence their skin is less susceptible to photoaging than that of males. We expect that the age dependence of SHG images in female subjects will reflect the effect of intrinsic aging on dermal collagen fiber more clearly, without a little interference by photoaging.

3.2 *Influence of UV Exposure History on Facial Collagen Fiber at Different Ages*

We investigated how cumulative UV exposure influences facial collagen fibers at different ages. Here we compared SHG images of facial collagen fibers between male subjects in their 20s with and without a recent life history of excessive sun exposure. Figure 4(a) and 4(b) shows photographs of the cheek skin (image size = 58×43 mm) and large-area SHG images (image size = 2.4×2.4 mm) of two subjects in their 20s, subject D with excessive sun exposure and subject E with moderate sun exposure. We confirmed again that thin collagen fibers were densely distributed in both skins, which is characteristic in young subjects. Furthermore, thin collagen fibers in subject D with excessive sun exposure were somewhat less abundant than those in subject E with moderate sun exposure, whereas thick collagen fibers in the former were slightly more conspicuous than those in the latter. However, it was difficult to find clear differences in collagen fiber structure between them.

Next we compared two subjects in their 50s, subject J with a life history of excessive sun exposure and subject K with moderate sun exposure, as shown in Fig. 5(a) and 5(b). In contrast to the subjects in their 20s, we confirmed a large difference in facial collagen fibers between the two subjects. Subject J with excessive sun exposure in Fig. 5(a) showed drastically reduced thin collagen fibers, which had almost completely disappeared, except in areas around pores, whereas a small amount of thick collagen fibers remained. On the other hand, in subject K with moderate sun exposure in Fig. 5(b), both thin and thick collagen fibers still remained. Thus structural differences in collagen fiber due to UV effect were enhanced in the subjects in their 50s compared with the subjects in their 20s.

We here discuss the reason why the structures of the facial collagen fibers are so different between the subjects. UV irradiation to the skin inhibits the synthesis of collagen and induces its degradation.[32,33] At the same time, UV irradiation induces

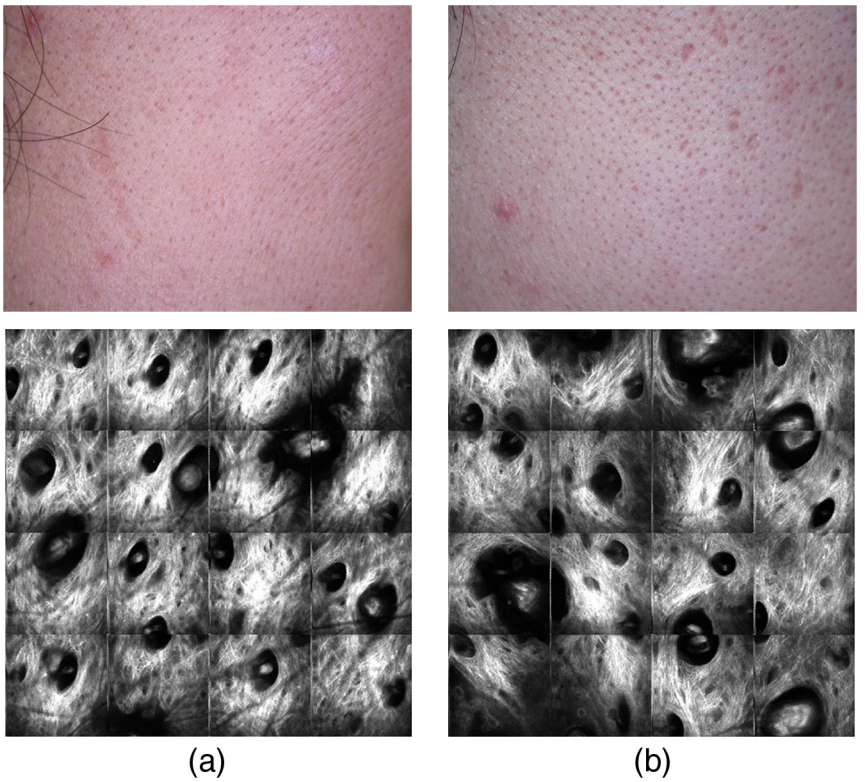

Fig. 4 Comparison of photographs of the cheek skin and large-area SHG images between subjects in their 20s with and without a recent life history of excessive sun exposure. (a) Subject D with excessive sun exposure and (b) subject E with moderate sun exposure.

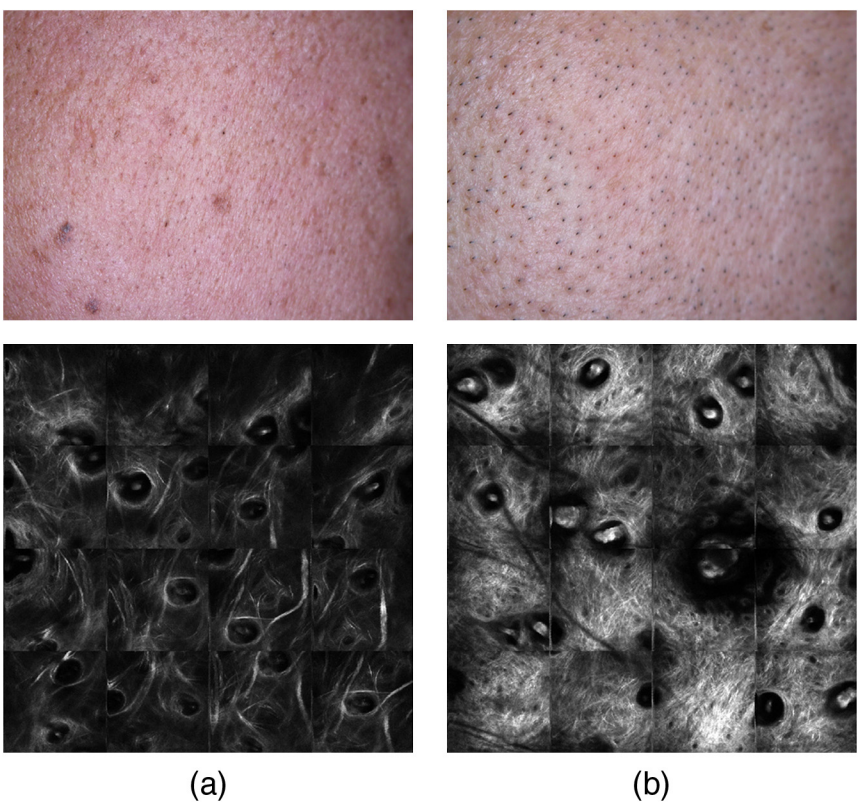

Fig. 5 Comparison of photographs of the cheek skin and large-area SHG images between subjects in their 50s with and without a recent life history of excessive sun exposure. (a) Subject J with excessive sun exposure and (b) subject K with moderate sun exposure.

elastin gene transcriptional activity, resulting in increased deposition of elastin that replaces the degenerated collagen, referred to as solar elastosis.[5] On the other hand, intrinsic aging diminishes collagen synthesis, resulting in the decreased density of collagen fiber in the dermis as shown in Fig. 2(e). Therefore, UV irradiation to intrinsically aged skin makes it easier to change the ratio of the degenerated collagen to the abnormal elastin. The SHG images sensitively reflect the fact that a combination of photoaging with intrinsic aging greatly accelerates skin aging.

Since the elastin fibers induce third harmonic generation (THG) light under the illumination of a Cr:F laser,[34] the combined microscopy of SHG and THG may give the detailed insight regarding the collagen/elastin ratio as well as the combined microscopy of collagen-specific SHG and elastin-specific TPF.[19–21] To visualize the distribution of dermal collagen and elastin fibers in the photoaged skin, we performed simultaneous SHG and THG imaging by incorporating an additional PMT with a bandpass filter suitable for THG light. Figure 6(a) and 6(b) shows collagen-specific SHG image (observed wavelength = 608 to 646 nm) and elastin-specific THG image (observed wavelength = 385 to 444 nm) of a subject in his 50s with a life history of excessive sun exposure (subject J). We were expecting that the elastin-specific THG signal was observed only in the area where the collagen-specific SHG signal was not observed, namely, the complementary distribution of elastin-specific THG signal to collagen-specific SHG signal. However, actual THG signal is weak in the whole region of Fig. 6(b), whereas coarse distribution of thick collagen fibers was clearly visualized in SHG image of Fig. 6(a). Considering that the change of the collagen/elastin ratio was confirmed in the previous studies based on combined SHG and TPF microscopy,[19–21] we can conclude that THG signal from the abnormal elastin is too weak to detect it in the present setup, or the abnormal elastin does not induce THG light.

One might consider that the reason for the structural difference in the subjects in their 50s (see Fig. 5) is to make the comparison at different relative depth due to intrinsic aging-related thinning and/or photoaging-related thickening of the epidermis because the collagen structures changes with depth. In this case, depth-resolved SHG imaging will provide more information of those structural changes in dermal collagen. Therefore, we performed depth-resolved SHG imaging for these subjects in their 50s. The resulting series of depth-resolved SHG images are shown in Fig. 7 (imaged region = 600×600 μm, interval of scanning depth = 10 μm), where the surface of skin is defined as a depth of 0 μm. In the case of subject J with excessive sun exposure in Fig. 7(a), nonfibrous structures were observed within a range of depths from 60 to 100 μm and then disappeared at a depth of 110 μm. We consider that these SHG images were also contaminated by other signals due to imperfect blocking of the infrared-cut filter (pass wavelength <800 nm). Endogenous chromospheres in the epidermis, such as NAD(P)H, FAD, retinol, tryptophan, and keratin emit autofluorescence signal via multiphoton process.[16,17,30] Furthermore, local optical inhomogeneities in the epidermis cause THG signal.[26–28] At the present time, although it is still difficult to specify the source of this faint signal, this faint SHG signal may give an indicator related with the photoaging. Work is in progress to specify it. At a depth of 120 μm, thick collagen fiber in the reticular dermis appeared; however, it immediately disappeared at a depth of 140 μm. At a depth of 150 μm, even thick collagen fibers greatly decreased. Conversely, in the case of subject K with moderate sun exposure in Fig. 7(b), thin collagen fibers in the papillary dermis were observed between depths of 50 and 70 μm, and thick collagen fibers were observed in the reticular dermis at depths over 80 μm. These results show the age-related structural changes in dermal collagen fibers progress in the depth direction, in addition to the lateral distribution.

3.3 *Image Analysis Based on Fourier Transform*

The collagen-sensitive SHG microscope could visualize age-related structural changes in dermal collagen fibers in the form of high-contrast SHG images. If a skin aging parameter can be extracted only from the SHG signal without the help of elastin-specific TPF signal, *in vivo* assessment of human skin aging will be simplified. We next considered how to extract a quantitative parameter related to skin aging from those SHG images.

The intensity value in an SHG image is often influenced by the conditions of the laser source, the scattering efficiency in the epidermis layer, and other factors, although it can give us information about the level of structural maturity and density of dermal collagen. One potential method to extract an aging parameter from the present SHG images is to use image analysis, because structural changes in the dermal collagen fibers were clearly visualized as image differences. Recently, image analysis based on Fourier transformation has been used for

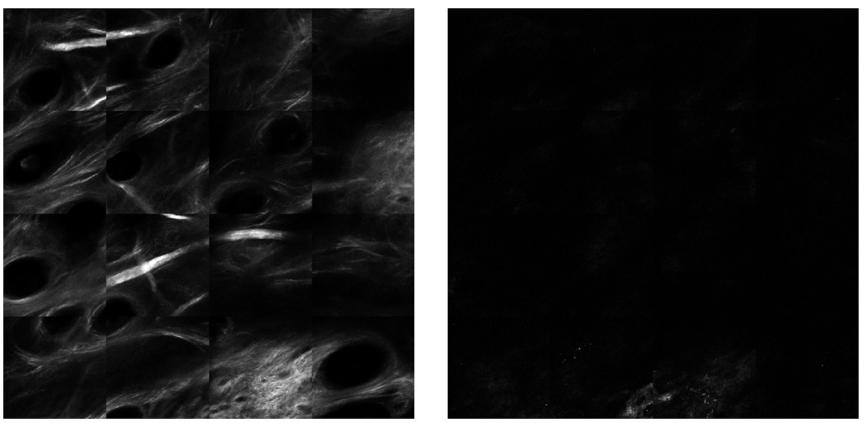

Fig. 6 Comparison of (a) collagen-specific SHG image and (b) elastin-specific THG image for subject J with excessive sun exposure.

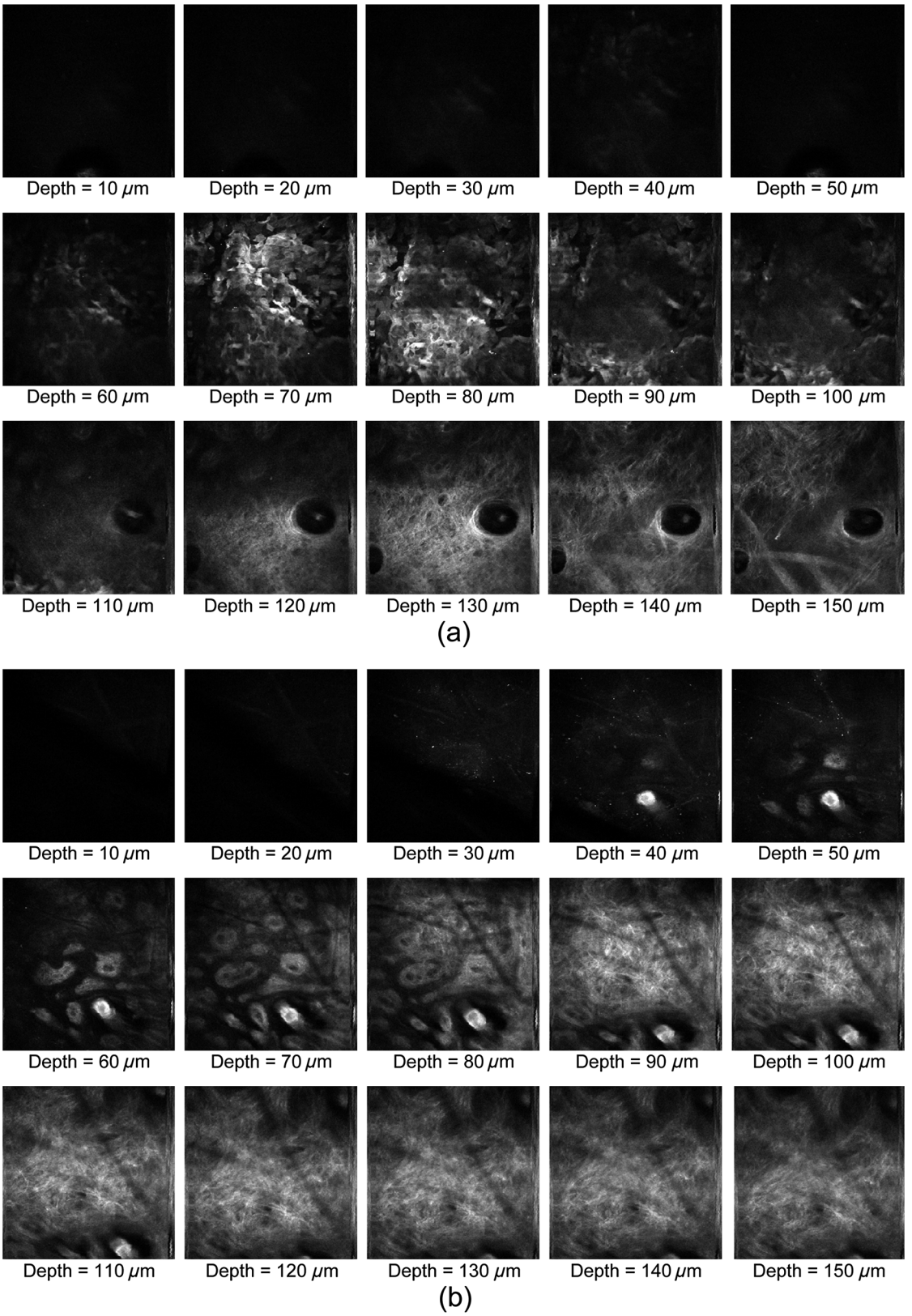

Fig. 7 Comparison of depth-resolved SHG images between subjects in their 50s with and without a recent life history of excessive sun exposure. (a) Subject J with excessive sun exposure and (b) subject K with moderate sun exposure.

SHG images in order to assess the structure of collagen fibers.[35,36] We tried to extract a quantitative parameter related to this difference from SHG images by using Fourier transform (FT) analysis of the images.

We analyzed SHG images of dermal collagen fibers based on the following procedure. First, we selected region of interest (ROI; size $= 64 \times 64$ pixels) so that the ROI did not include pores. Second, we performed 2-D FT of the selected ROI

and obtained the FT spectrum of it. Third, we fitted a Gaussian function to the spectral shape to determine its spectral width [full width at half maximum (FWHM)]. We consider that this FT spectral width can be used for an indicator reflecting the difference of spatial distribution in dermal collagen fiber. Finally, after applying the above procedure for five different ROIs in the same subject, we calculated the mean and standard deviation of the spectral width.

Figure 8 shows a comparison of the spectral widths for all subjects. In the case of subjects A, B, and E who indicated dense distributions of thin collagen fibers, the spectral widths were relatively narrow. Conversely, subjects J and L, indicating coarse distributions of thick collagen fibers owing to intrinsic aging and/or photoaging, had particularly wide spectral widths. Furthermore, relatively speaking, the spectral widths increased in proportion to age. These tendencies well reflected the characteristic structures of dermal collagen fibers in the nonaging and aging skins, although we could not perform the statistical analysis of this parameter due to the limited number of subjects in this experiment. We here consider the correlation between the qualitative and the quantitative results of SHG images, although it is difficult to obtain the clear interpretation for the correlation due to less spatial periodicity of collagen fibers. In the case of young subjects, SHG images were obtained at low contrast due to dense distributions of thin collagen fibers. On the other hand, elderly subjects indicated high-contrast SHG images due to coarse distributions of thick collagen fibers. We consider that difference of the image contrast influences FT spectral width. In other words, harmonic components of the fundamental spatial frequencies were enhanced by the high image contrast, leading to the increase of FT spectral width. At the present stage, although this only-SHG-based parameter just shows a possibility as the aging parameter, it may enable simpler assessment of human skin aging than conventional parameters based on combination of collagen-specific SHG signal and elastin-specific TPF signal.[19–21] Work is in progress to evaluate this parameter from the viewpoint of the statistical analysis by increasing the number of subjects. In addition to FT analysis of SHG image, combination of SHG microscopy with the polarization measurement, namely polarization-resolved SHG microscopy, may also give an additional means for the skin-aging parameter based only on SHG signal because the skin wrinkling, characteristic in the aged skin, is closely related with orientation of collagen fiber.[29]

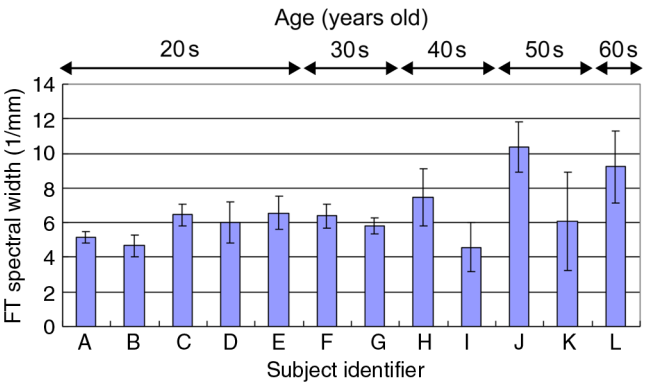

Fig. 8 Comparison of FT spectral widths for all subjects.

4 Conclusions

We evaluated the potential of a collagen-sensitive SHG microscope equipped with a Cr:Forsterite laser as an *in vivo* assessment tool for skin aging from the viewpoint of structural changes in dermal collagen fibers. Ability to probe deeper below skin surface in this SHG microscope enables us to visualize age-related structural change of collagen fiber in the reticular dermis clearly. SHG images of human facial skin clearly visualized age-related structural changes in dermal collagen fibers: young subjects showed dense distributions of thin collagen fibers, whereas elderly subjects showed coarse distributions of thick collagen fibers. Furthermore, a comparison of SHG images between subjects in their 50s with and without a recent life history of excessive sun exposure showed that a combination of photoaging with intrinsic aging significantly accelerates skin aging. Such age-related structural change of dermal collagen was also confirmed in depth-resolved SHG imaging. Finally, to extract a quantitative parameter related to skin aging from SHG images, we defined the spectral width of an FT spectrum of SHG image as an aging parameter. The FT spectral width moderately reflected age-related structural change of dermal collagen. Therefore, the collagen-sensitive SHG microscope will be a powerful tool of *in vivo* skin assessment in fields such as anti-aging dermatology and the development of skin cosmetics.

Acknowledgments

This work was supported by Grants-in-Aid for Scientific Research Nos. 22300154, 23240069, and 23650260 from the Ministry of Education, Culture, Sports, Science, and Technology of Japan. We are grateful to Dr. Mamoru Hashimoto of Osaka University for fruitful discussions.

References

1. B. A. Gilchrest, "Skin aging and photoaging: an overview," *J. Am. Acad. Dermtol.* **21**(3), 610–613 (1989).
2. M. El-Domyati et al., "Intrinsic aging vs. photoaging: a comparative histopathological, immunohistochemical, and ultrastructural study of skin," *Exp. Dermatol.* **11**(5), 398–405 (2002).
3. M. A. Farage et al., "Intrinsic and extrinsic factors in skin ageing: a review," *Int. J. Cosmet. Sci.* **30**(2), 87–95 (2008).
4. J. Varani et al., "Decreased collagen production in chronologically aged skin: roles of age-dependent alteration in fibroblast function and defective mechanical stimulation," *Am. J. Pathol.* **168**(6), 1861–1868 (2006).
5. T. Quan et al., "Matrix-degrading metalloproteinases in photoaging," *J. Invest. Dermatol. Symp. Proc.* **14**(1), 20–24 (2009).
6. H. S. Talwar et al., "Reduced type I and type III procollagens in photodamaged adult human skin," *J. Invest. Dermatol.* **105**(2), 285–290 (1995).
7. C. E. Griffiths, "The clinical identification and quantification of photodamage," *Br. J. Dermatol.* **127**(S41), 37–42 (1992).
8. V. Siskind et al., "Sun exposure and interaction with family history in risk of melanoma, Queensland, Australia," *Int. J. Cancer* **97**(1), 90–95 (2002).
9. C. Kennedy et al., "The influence of painful sunburns and lifetime sun exposure on the risk of actinic keratoses, seborrheic warts, melanocytic nevi, atypical nevi, and skin cancer," *J. Invest. Dermatol.* **120**(6), 1087–1093 (2003).
10. S. C. Thompson, D. Jolley, and R. Marks, "Reduction of solar keratoses by regular sunscreen use," *N. Engl. J. Med.* **329**(16), 1147–1451 (1993).
11. P. K. Vayalil et al., "Green tea polyphenols prevent ultraviolet light-induced oxidative damage and matrix metalloproteinases expression in mouse skin," *J. Invest. Dermatol.* **122**(6), 1480–1487 (2004).

12. M. C. Branchet et al., "Morphometric analysis of dermal collagen fibers in normal human skin as a function of age," *Arch. Gerontol. Geriatr.* **13**(1), 1–14 (1991).
13. A. Yariv, *Introduction to Optical Electronics*, Holt McDougal, Geneva (1977).
14. I. Freund, M. Deutsch, and A. Sprecher, "Connective tissue polarity. Optical second-harmonic microscopy, cross-beam summation, and small-angle scattering in rat-tail tendon," *Biophys. J.* **50**(4), 693–712 (1986).
15. P. J. Campagnola and C.-Y. Dong, "Second harmonic generation microscopy: principles and applications to disease diagnosis," *Laser Photon. Rev.* **5**(1), 13–26 (2011).
16. J. A. Palero et al., "*In vivo* nonlinear spectral imaging in mouse skin," *Opt. Express* **14**(10), 4395–4402 (2006).
17. K. König and I. Riemann, "High-resolution multiphoton tomography of human skin with subcellular spatial resolution and picosecond time resolution," *J. Biomed. Opt.* **8**(3), 432–439 (2003).
18. K. König et al., "Current developments in clinical multiphoton tomography," *Proc. SPIE* **7569**, 756915 (2010).
19. S.-J. Lin et al., "Evaluating cutaneous photoaging by use of multiphoton fluorescence and second-harmonic generation microscopy," *Opt. Lett.* **30**(17), 2275–2277 (2005).
20. M. J. Koehler et al., "*In vivo* assessment of human skin aging by multiphoton laser scanning tomography," *Opt. Lett.* **31**(19), 2879–2881 (2006).
21. S. Puschmann et al., "Approach to quantify human dermal skin aging using multiphoton laser scanning microscopy," *J. Biomed. Opt.* **17**(3), 036005 (2012).
22. I.-H. Chen et al., "Wavelength dependent damage in biological multi-photon confocal microscopy: a micro-spectroscopic comparison between femtosecond Ti:sapphire and Cr:forsterite laser sources," *Opt. Quantum Electron.* **34**(12), 1251–1266 (2002).
23. S.-W. Chu et al., "*In vivo* developmental biology study using noninvasive multi-harmonic generation microscopy," *Opt. Express* **11**(23), 3093–3099 (2003).
24. S.-P. Tai et al., "*In vivo* optical biopsy of hamster oral cavity with epi-third-harmonic-generation microscopy," *Opt. Express* **14**(13), 6178–6187 (2006).
25. T. Yasui et al., "*Ex vivo* and *in vivo* second-harmonic-generation imaging of dermal collagen fiber in skin: comparison of imaging characteristics between mode-locked Cr:Forsterite and Ti:Sapphire lasers," *Appl. Opt.* **48**(10), D88–D95 (2009).
26. C.-K. Sun et al., "Multiharmonic-generation biopsy of skin," *Opt. Lett.* **28**(24), 2488–2490 (2003).
27. S.-P. Tai et al., "Optical biopsy of fixed human skin with backward-collected optical harmonics signals," *Opt. Express* **13**(20), 8231–8242 (2005).
28. S.-Y. Chen, H.-Y. Wu, and C.-K. Sun, "*In vivo* harmonic generation biopsy of human skin," *J. Biomed. Opt.* **14**(6), 060505 (2009).
29. T. Yasui et al., "Observation of dermal collagen fiber in wrinkled skin using polarization-resolved second-harmonic-generation microscopy," *Opt. Express* **17**(2), 912–923 (2009).
30. A.-M. Pena et al., "Spectroscopic analysis of keratin endogenous signal for skin multiphoton microscopy," *Opt. Express* **13**(16), 6268–6274 (2005).
31. C. Longo et al., "Skin aging: *in vivo* microscopic assessment of epidermal and dermal changes by means of confocal microscopy," *J. Am. Acad. Dermatol.* (in press).
32. G. J. Fisher et al., "Pathophysiology of premature skin aging induced by ultraviolet light," *N. Engl. J. Med.* **337**(20), 1419–1428 (1997).
33. G. J. Fisher et al., "c-Jun-dependent inhibition of cutaneous procollagen transcription following ultraviolet irradiation is reversed by all-trans retinoic acid," *J. Clin. Invest.* **106**(5), 663–670 (2000).
34. C.-K. Sun et al., "*In vivo* and *ex vivo* imaging of intra-tissue elastic fibers using third-harmonic-generation microscopy," *Opt. Express* **15**(18), 11167–11177 (2007).
35. R. A. Rao, M. R. Mehta, and K. C. Toussaint, "Fourier transform-second-harmonic generation imaging of biological tissues," *Opt. Express* **17**(17), 14534–14542 (2009).
36. M. Sivaguru et al., "Quantitative analysis of collagen fiber organization in injured tendons using Fourier transform-second harmonic generation imaging," *Opt. Express* **18**(24), 24983–24993 (2010).